# Palladium nanostructures synthesized by radiolysis or by photoreduction†

**Tanafit Redjala,[a] Gabriela Apostolecu,[a] Patricia Beaunier,[b] Mehran Mostafavi,[a] Arnaud Etcheberry,[c] Denis Uzio,[d] Cécile Thomazeau[d] and Hynd Remita*[a]**

***Received (in Montpellier, France) 19th December 2007, Accepted 25th February 2008***
***First published as an Advance Article on the web 15th April 2008***
**DOI: 10.1039/b719517f**

Palladium nanostructures formed by nanowires, nanoplates or having a flower-like shape were synthesized by slow reduction *via* radiolysis or *via* photoreduction of palladium acetylacetonate $Pd(acac)_2$ in 2-propanol under CO atmosphere.



## 1 Introduction

Nanostructured metals are attracting much attention because of their potential applications in catalysis,[1] electronics,[2,3] and optics.[4] The synthesis of well-controlled shapes and sizes of nanoparticles and nanomaterials is often critical for their performances[5] as it is the case in catalysis or electro-catalysis where the activity strongly depends on the size and shape of the metal nanoparticles.[6–9]

Palladium is one of the most efficient metals in catalysis, especially for the formation of C–C bonds[10] in organic reactions such as Suzuki, Heck and Stille coupling[11–15] and for the hydrogenation of polyunsaturated hydrocarbons.[16,17] Palladium is also known as an efficient electro-catalyst for ethanol oxidation for fuel cell applications[18,19] and also displays a remarkable performance in $H_2$ storage and sensing.[20]

It has been shown that the catalytic activity of platinum and palladium nanostructures highly depends on the morphology of the nanoparticles.[9,21] Pd nanoparticles of different sizes and morphologies have been synthesized in the presence of ligands, surfactants or polymers.[22] Hexagonal plates and cubic particles of Pd have been obtained *via* RNA-mediated growth control.[23] Xia and co-workers have synthesized Pd triangles and nanoplates by the polyol process and have shown that these nanostructures are active substrates for surface-enhanced Raman scattering (SERS).[24] Rectangular palladium nanoparticles have been recently obtained *via* the reduction of $Pd^{II}$ by ascorbic acid in the presence of a surfactant, cetyltrimethylammonium bromide and trisodium citrate.[25] Arrays of palladium nanostructures have been synthesized using mesoporous silica (MCM-48 and SBA-15) as templates by chemical vapour infiltration,[26] and the ball-shaped palladium nanocatalysts Pd@MCM-48 present remarkable selectivity for the cleavage of benzyl ethers, demonstrating that nanostructured mesoporous materials exhibit interesting catalytic activity through cooperative properties.[27]

Radiolytic reduction is a powerful method to synthesize metallic nanoparticles and nanostructures.[28–31] The specificity of the radiation-induced reduction of metal ions into atoms lies in generating radiolytic species of strongly reducing potential. The final structure and size of the nanoparticles result from the growth process which can be controlled by the nature of the stabilizers (ligands, surfactants or polymers), the salt and stabilizer concentrations, and the dose rate. In particular, we have shown that the dose rate, which fixes the reduction kinetics, has an effect on the mean size and the structure of the nanoparticles formed by irradiation.[32–34] The kinetic control of the reduction and growth processes is critically important to control the nanoparticle size and shape.

Photoreduction of metal salts in solutions or in soft or hard templates is also an efficient way to synthesize metal nanoparticles or nanostructures.[35–38]

Herein, we describe the synthesis of 1D, 2D and 3D Pd nanostructures by radiolysis or by photoreduction in 2-propanol solution under CO atmosphere. New Pd flower-like nanostructures comprised of thin foils as well as hexagonal nanoplates and nanowires were obtained.

## 2 Experimental

Solutions of $Pd(acac)_2$ (purchased from Johnson Matthey) in pure 2-propanol (concentration range: $1 \times 10^{-4}$ to $2 \times 10^{-3}$ mol $L^{-1}$) were transferred in small Pyrex flasks closed with a rubber plastic septum and were carefully degassed and saturated with carbon monoxide (purchased from Air Liquide) at atmospheric pressure by CO bubbling during 15 min. As CO is very toxic, CO bubbling was achieved with high caution in a well-ventilated hood with external evacuation for CO. The $Pd(acac)_2$ solutions were irradiated quickly after CO bubbling in order to avoid the direct very slow reduction of $Pd^{II}$ by CO which induces the formation of large black particles after several days.

The γ-irradiation source was a $^{60}Co$ gamma-facility of 7000 Curies with a dose rate of 3000 Gy $h^{-1}$ at Orsay. Electron beam irradiations were performed with a 20 kW and 10 MeV electron accelerator (CARIC-Ionisos Society) delivering trains

[a] *Laboratoire de Chimie Physique, Université Paris XI, UMR 8000-CNRS, Bât. 349, 91405 Orsay, France. E-mail: hynd.remita@lcp.u-psud.fr; Fax: (+33) (0)1 69 15 30 55; Tel: (+33) (0)1 69 15 72 58*
[b] *Laboratoire de Réactivité de Surface, Université Paris-VI, UMR 7609-CNRS, 4 Place Jussieu, 75252 Paris Cedex 05, France*
[c] *Institut Lavoisier de Versailles, Université Versailles Saint-Quentin-en-Yvelines, UMR 8180-CNRS, 45 ave des Etats-Unis, 78035 Versailles Cedex, France*
[d] *IFP, Direction Catalyse & Séparation, IFP-Lyon, BP no 3, 69390 Vernaison, France*

† Electronic supplementary information (ESI) available: Fig. S1: Absorption spectrum evolution with UV irradiation of a solution containing $10^{-3}$ mol $L^{-1}$ $Pd(acac)_2$ in 2-propanol under 1 atm of CO. See DOI: 10.1039/b719517f

of 14 μs pulses (10–350 Hz) through a scanning beam (1–10 Hz) of mean dose rate 2200 Gy $s^{-1}$ (7.9 MGy $h^{-1}$). For those experiments the solutions were irradiated in glass vessels with a rubber plastic septum.

For photoreduction, $Pd(acac)_2$ solutions were irradiated in quartz cells under CO atmosphere with an Oriel 300 W Xenon UV-visible lamp.

UV-visible absorption spectra were recorded with a double beam Perkin Elmer Lambda 19 spectrophotometer.

Transmission electron microscopy (TEM) observations were performed with a JEOL 100CXII transmission electron microscope at an accelerating voltage of 100 kV and for high-resolution measurements with a JEOL JEM 2010 at 200 kV. Drops of the irradiated solutions were deposited on carbon-coated copper grids and dried under $N_2$ flow.

The XPS analysis was performed on In foils. Sample drops were deposited on the foils and dried under $N_2$ flow. The XPS analyzer was a Thermo Electron ESCALAB 220i-XL. Either a non-monochromatic or a monochromatic X-ray Al-Kα line was used for excitation. The photoelectrons were detected perpendicularly to the support. A constant analyzer energy mode was used with pass energy of 20 eV.

## 3 Results and discussion

### Radiolytic synthesis

2-Propanol solutions containing $Pd^{II}(acac)_2$ were irradiated under CO atmosphere. $Pd^{II}$ can be reduced by solvated electrons and 2-propanol radicals $(CH_3)_2$–$C^{\bullet}OH$[39–41] produced by the solvent radiolysis and by $CO^-$ formed by the fast reaction of CO with solvated electrons ($k = 2.8 \times 10^9$ L $mol^{-1}$ $s^{-1}$ in ethanol).[42] The solutions after irradiation under CO are dark blue.

With increasing irradiation dose, the peak at 326 nm associated with the $Pd^{II}(acac)_2$ complex decreases in intensity and a new band appears at 275 nm (Fig. 1). Three quasi-isosbestic points are found at around 255, 310 and 335 nm. The surface plasmon spectra of spherical palladium nanoparticles are known to exhibit a resonance band in the UV range at around 205 nm. In addition to this plasmon band, a broad absorption in the region 400–1200 nm is observed with highest absorbance in the infrared. The absorption band obtained at 275 nm is due to free acetylacetone.

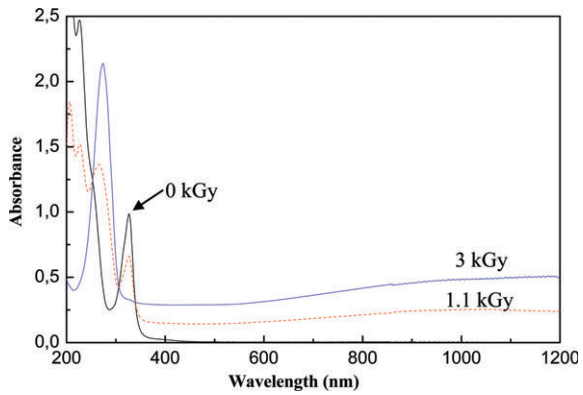


**Fig. 1** Absorption spectrum evolution with γ-irradiation dose of a solution containing $10^{-3}$ mol $L^{-1}$ $Pd(acac)_2$ in 2-propanol under 1 atm of CO. Dose rate 3 kGy $h^{-1}$. Optical path = 1 mm.

The solutions containing $Pd^{II}(acac)_2$ are stable under CO for many hours: there is no evolution of the absorption spectrum and large black Pd particles (which precipitate) appear only after a few days. This indicates that, at room temperature and under our conditions of concentrations, CO reduces $Pd^{II}$ very slowly and the direct reduction by CO is negligible at the scale of hours.

The radiolytic reduction of $Pd^{II}(acac)_2$ at $10^{-3}$ mol $L^{-1}$ in 2-propanol under CO atmosphere leads to Pd nanostructures. Fig. 2 shows TEM images of the samples at different doses and their corresponding selected area electron diffraction (SAED) pattern. These Pd nanostructures are composed of thin crumpled foils (50–100 nm large) with a few nanowires as shown in Fig. 2(c) and (d). At the end of reduction (3 kGy corresponding to 1 h irradiation), these nanostructures appear as flower-like structures with a core from which different foils spread out. A few individual nanoplates are also observed (Fig. 2(c)). The formation of the plates is observed at low dose. Different foils seem to originate from the same seed. It is known that nanoplates exhibit surface plasmon features different from those of cuboctahedra or twinned nanoparticles. Pd nanodisks exhibit broad localized surface plasmons with higher sensitivity of the plasmon to the disk ratio compared to Ag.[43] Xia and co-workers[24] reported a broad peak at 530 nm for Pd nanoplates. The broadness of the peak has been attributed to the dielectric function of Pd and to the low thickness of the plates.

At lower concentration of $Pd^{II}$ complex ($10^{-4}$ mol $L^{-1}$), as shown in Fig. 3, more elongated nanostructures with more thin nanowires are obtained. The diameter of the nanowires is 2 nm and their length lies between a few nm to 100 nm. The selected area electron diffraction (SAED) from a region of the TEM image shows a ring-like pattern indicating a polycrystalline structure (Fig. 3(a) inset). At higher magnification, high-resolution (HRTEM) micrographs confirm that the Pd nanostructures and nanowires are crystalline (Fig. 3(c)). The fast Fourier transformation (FFT) of this image reveals one main diffraction ring and two symmetric points (Fig. 3(c) inset). The reciprocal distances found, $d_1 = 0.225$ nm and $d_2 = 0.198$ nm, correspond to the (111) and (200) planes lattice of cubic Pd.

XPS analysis shows that the Pd nanostructures (obtained at $10^{-3}$ or $10^{-4}$ mol $L^{-1}$ $Pd^{II}$) exhibit two reproducible peaks (at 335.68 and 340.94 eV), features which are specific to the $3d_{5/2}$/$3d_{3/2}$ spin–orbit splitting. The asymmetric shape of each contribution is always present which agrees with the metallic character of the Pd nanoparticles and completes the information given by the binding energy positions (Fig. 4). However a small additional Pd $3d_{3/2}$/$3d_{5/2}$ contribution at 336.92 and 342.49 eV must be added to achieve a good simulation. This high energy contribution can be interpreted as resulting from a thin film coverage by acetylacetone (which is a versatile ligand)[44] or CO.[45] Both electron diffraction and XPS analysis of dried samples confirm that the nanostructures are composed of completely reduced palladium.[46] It should be noted that these structures are stable in solution under CO over weeks as proved by microscopy and XPS measurements.

The same solutions, when irradiated with gamma rays under $N_2$ atmosphere, are brown. The shape of the final absorption

 

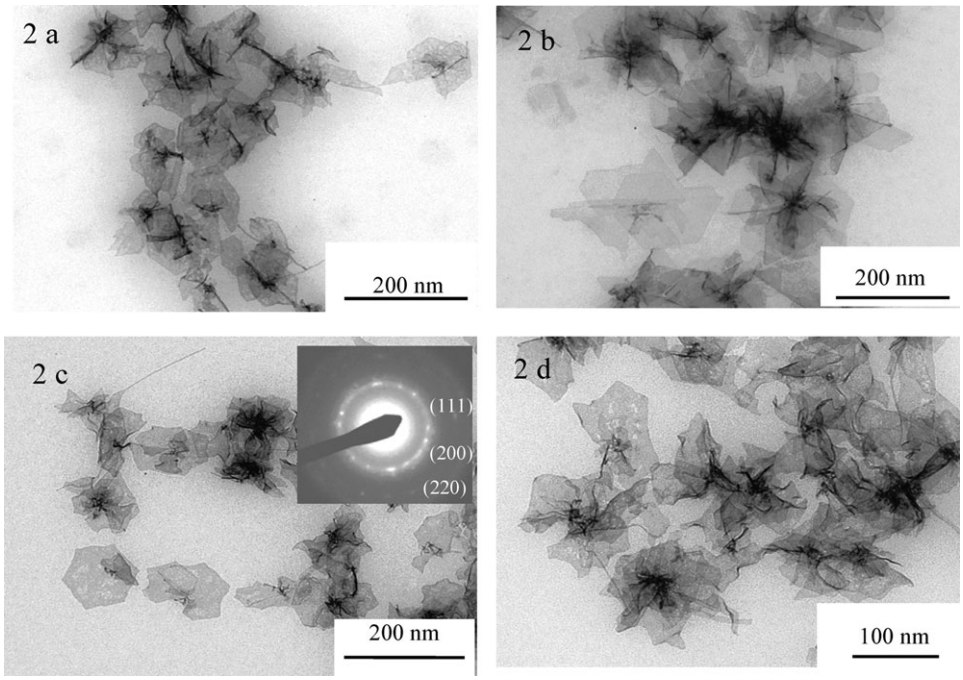


**Fig. 2** TEM micrographs of Pd nanostructures obtained by γ-irradiation (dose rate: 3 kGy $h^{-1}$) of a solution containing $10^{-3}$ mol $L^{-1}$ $Pd(acac)_2$ in 2-propanol under CO atmosphere: (a) dose = 0.5 kGy, (b) dose = 1.4 kGy, (c, d) dose = 3.6 kGy. The inset to (c) shows the indexed corresponding SAED pattern.

spectrum below 350 nm is very similar in the UV region to that obtained under CO but no absorption is observed above 400 nm. In the presence of $N_2$, 2 nm spherical particles were obtained (as shown in Fig. 5(a)) indicating the importance of

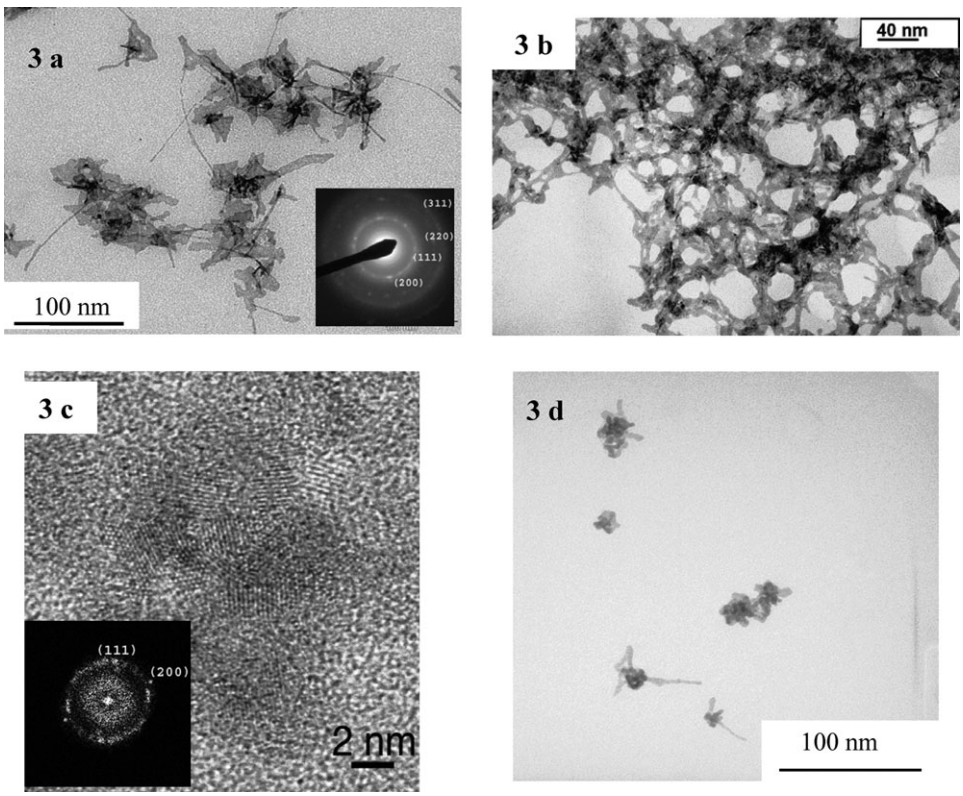


**Fig. 3** TEM micrographs of Pd nanostructures obtained by γ-irradiation (dose rate: 3 kGy $h^{-1}$, dose: 360 Gy) (a–c) or by photoreduction (2 h) (d) of a solution containing $10^{-4}$ mol $L^{-1}$ $Pd(acac)_2$ in 2-propanol under CO atmosphere. (a) Inset: the indexed SAED pattern. (c) High-resolution micrograph of the Pd nanostructures obtained under CO atmosphere and inset the corresponding fast Fourier transformation (FFT).

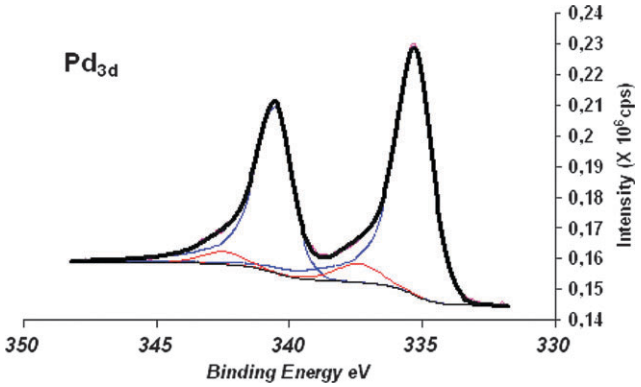


**Fig. 4** XPS signals of the Pd nanostructures deposited on In foils and obtained by γ-irradiation of 2-propanol solutions of $Pd^{II}(acac)_2$ ($10^{-3}$ mol $L^{-1}$) under CO atmosphere, dose = 3 kGy. The thick black line corresponds to the $Pd_{3d}$ experimental signal and the thin black line is the Shirley background. The experimental signal is fitted by two double (3/2–5/2) components. The low binding energy (LE) components (--, blue) are constructed using an asymmetric shape with the parameters of a metallic Pd standard while the high energy (HE) components (-·-, red) are constructed with a symmetrical shape; the area ratio $Pd_{HE}/Pd_{LE}$ is 0.08.

CO in the formation of the new Pd nanostructures as previously described.

Fast radiolytic reduction of $Pd^{II}$ $(acac)_2$ in 2-propanol solution under CO atmosphere performed at much higher dose rate (accelerated electron source; dose rate: 7.9 MGy $h^{-1}$) leads to spherical particles with a narrow size distribution (diameter 2 nm). These observations show that the dose rate, which fixes the number of seeds and the reduction kinetics, has an influence on the structure growth. As for other face-centered cubic (fcc) noble metals, the thermodynamically favourable shapes of Pd nanocrystals are cuboctahedra and multiply twinned particles. The synthesis of Pd nanoplates or nanofoils requires the control of the reduction kinetics, particularly at the seeding stage.[47] Xia and co-workers have reported the formation of Pd nanoplates in a slow reduction process.[24] Silver triangles were also synthesized by slow reduction of $Ag^+$ by EDTA on radiolytically induced seeds.[48] Other literature results report the opposite process *i.e.* the formation of anisotropic nanostructures with a fast reduction process.[49] Here, it is clear that the presence of CO and the use of a low irradiation dose rate favour the formation of these anisotropic nanostructures.

### Synthesis by photoreduction

Similar experiments were conducted using slow photoreduction. TEM observations have shown Pd nanostructures formed by nanoplates or nanowires depending on the initial $Pd^{II}$ concentration. At $10^{-3}$ mol $L^{-1}$ of palladium under CO atmosphere, the complete photoreduction required 6 h and led to palladium foils arising from the same core (Fig. 6(a)) or to individual nanoplates with regular mainly hexagonal shapes (Fig. 6(b) and (c)). These hexagonal platelets (70–100 nm) are mono-crystalline and the ED pattern (Fig. 6(c) inset) shows six-fold symmetry of the diffraction spots indicating that the hexagonal faces are composed by

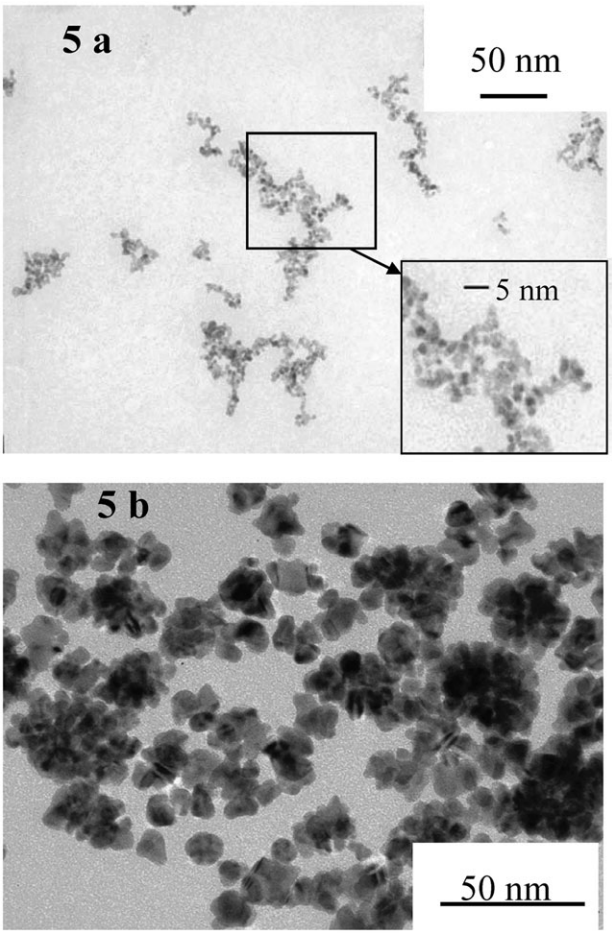


**Fig. 5** TEM micrographs of Pd nanoparticles obtained by γ-radiolysis (dose = 3.6 kGy) (a) or by photoreduction (5 h irradiation) (b) of a solution containing $10^{-3}$ mol $L^{-1}$ $Pd(acac)_2$ in 2-propanol under $N_2$ atmosphere. The inset of (a) shows a magnified image where the 2 nm Pd particles are clearly seen.

(111) planes.[50] The borders appear sometimes as a rolling up of the nanoplates. In this case, the selected area electron diffraction presents an additional distance consistent with the (200) plane lattice of Pd (Fig. 6(c) inset). Other shapes such as triangles or truncated triangles and very few nanowires are also obtained (Fig. 6(d)). The XPS spectra of these nanoplates are similar to those of the nanostructures obtained by γ-radiolysis.

The spectrum evolution under UV-visible irradiation is close to that obtained with γ-radiolysis and the final spectrum shows a broad absorption from the visible to the infrared (400–1200 nm) (see Fig. S1 in ESI†).

The concentration of the Pd precursor has also an influence on the final structure: in the case of very dilute solutions ($10^{-4}$ mol $L^{-1}$) irradiated with UV light, more nanowires and fewer nanoplates are obtained (Fig. 3(d)).

The photoreduction of palladium under $N_2$ atmosphere leads to large nanoparticles of 8–10 nm as shown in Fig. 5(b) indicating that the presence of CO is necessary to obtain these 1D or 2D nanostructures.

Experiments are in progress to understand the growth process.

 

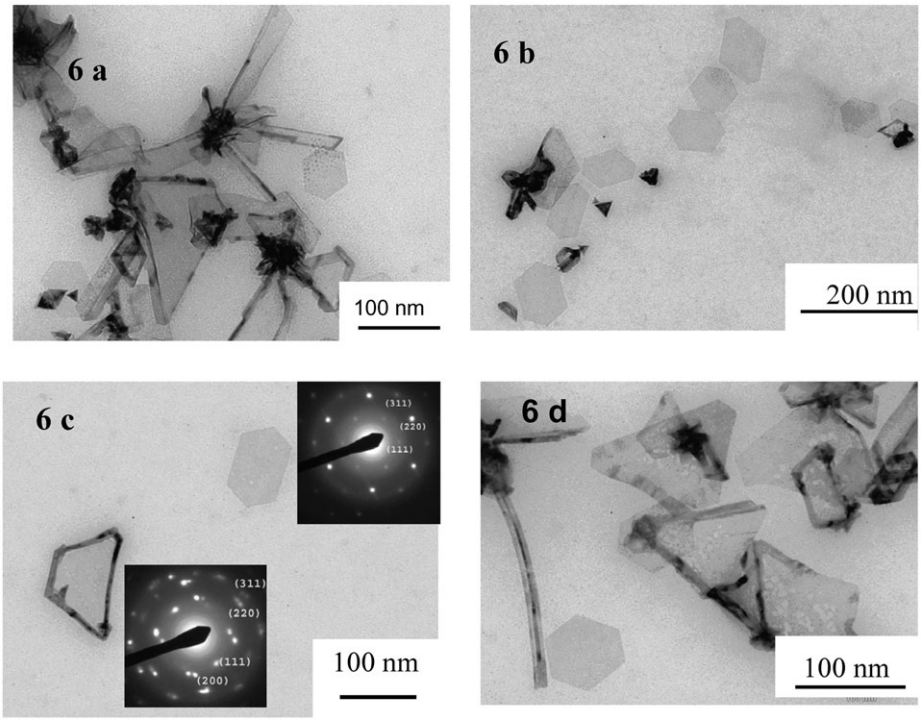


**Fig. 6** TEM micrographs (a–c) of Pd nanostructures obtained by photoreduction of $Pd^{II}$ in 2-propanol under CO atmosphere: $[Pd^{II}] = 10^{-3}$ mol $L^{-1}$, irradiation time 6 h. The inset to (c) shows the indexed SAED pattern of individual nanoplates. (d) $[Pd^{II}] = 10^{-4}$ mol $L^{-1}$, irradiation time 2 h.

## 4 Conclusion

Palladium nanostructures formed by nanowires, nanoplates or having a flower-like shape were synthesized by slow reduction either by photoreduction or by radiolysis of palladium acetylacetonate in 2-propanol under CO atmosphere. Upon fast radiolytic reduction with electron beams 2 nm nanoparticles were obtained. It is clear that the presence of CO and acac ligands and the reduction kinetics are key factors on the final structure. These new types of Pd nanostructures could find applications in different fields such as catalysis, electro-catalysis and SERS.

## Acknowledgements

The IFP is acknowledged for supporting this research. We also thank the European Commission for the fellowship awarded to Gabriela Apostolescu in the framework of the Marie Curie Training Site program (contract No HPT-CT-20000-00023). The authors thank Jackie Vigneron (Institut Lavoisier de Versailles) for his assistance for XPS experiments.

## References

1. (*a*) M. A. El-Sayed, *Acc. Chem. Res.*, 2001, **34**, 257; (*b*) G. Vitulli, P. Pertici, S. Bertozzi, C. Evangelisti, M. Vitulli, A. M. Caporusso and P. Salvadori, *Chim. Ind. (Milan)*, 2005, **87**, 64.
2. Y. Xia, P. Yang, Y. Sun, Y. Wu, B. Mayers, B. Gates, Y. Yan, F. Kim and H. Yan, *Adv. Mater.*, 2003, **15**, 353.
3. C. N. Rao, *Chem. Soc. Rev.*, 2000, **29**, 27.
4. S. A. Maier, P. G. Kik, H. A. Atwater, S. Meltzer, E. Harel, B. E. Koel and A. A. Requichia, *Nat. Mater.*, 2003, **2**, 229.
5. T. S. Ahmadi, Z. L. Wang, T. C. Green, A. Henglein and M. A. El-Sayed, *Science*, 1996, **272**, 1924.
6. W. M. H. Sachtler and R. A. van Santen, *Adv. Catal.*, 1977, **26**, 69.
7. J. A. Dalmon and G. A. Martin, *J. Catal.*, 1980, **66**, 214.
8. M. Che and C. O. Bennett, *Adv. Catal.*, 1989, **36**, 55.
9. C. Wang, H. Daimon, Y. Lee, J. Kimand and S. Sun, *J. Am. Chem. Soc.*, 2007, **129**, 6974.
10. D. Astruc, *Inorg. Chem.*, 2007, **46**, 1884.
11. M. T. Reetz and E. Westermann, *Angew. Chem., Int. Ed.*, 2000, **39**, 165.
12. R. Franzén, *Can. J. Chem.*, 2000, **78**, 957.
13. Y. Li, X. M. Hong, D. M. Collard and M. A. El-Sayed, *Org. Lett.*, 2000, **2**, 2385.
14. S.-W. Kim, M. Kim, W. Y. Lee and T. Hyeon, *J. Am. Chem. Soc.*, 2002, **124**, 7642.
15. S. U. Son, Y. Jang, J. Park, H. B. Na, H. M. Park, H. J. Yun, J. Lee and T. Hyeon, *J. Am. Chem. Soc.*, 2004, **126**, 5026.
16. T. Ouchaib, J. Massardier and A. Renouprez, *J. Catal.*, 1989, **119**, 517.
17. T. Redjala, H. Remita, G. Apostolescu, M. Mostafavi, C. Thomazeau and D. Uzio, *Gas Oil: Sci. Technol.*, 2006, **61**, 789.
18. S. S. Gupta and J. Datta, *J. Power Sources*, 2005, **145**, 124.
19. J. Liu, J. Ye, C. Xu, S. P. Jiang and Y. Tong, *Electrochem. Commun.*, 2007, **9**, 2334.
20. (*a*) P. Tobiska, O. Hugon, A. Trouillet and H. Gagnaire, *Sens. Actuators, A*, 2001, **74**, 168; (*b*) F. Favier, E. C. Walter, M. P. Zach, T. Benter and R. M. Penner, *Science*, 2001, **293**, 2227; (*c*) C. Langhammer, I. Zoric and B. Kasemo, *Nano Lett.*, 2007, **7**, 3122.
21. R. Narayanan and M. A. El-Sayed, *Nano Lett.*, 2004, **4**, 1343.
22. (*a*) E. Ramirez, S. Jansat, K. Philippot, P. Lacante, M. Gomez, A. M. Masdeu-Bulto and B. Chaudret, *J. Organomet. Chem.*, 2004, **689**, 4601; (*b*) J. S. Bradley, B. Tesche, W. Busser, M. Maase and M. T. Reetz, *J. Am. Chem. Soc.*, 2000, **122**, 4631; (*c*) T. Teranishi and M. Miyake, *Chem. Mater.*, 1998, **10**, 594; (*d*) S.-W. Kim, J. Park, Y. Jang, Y. Chung, S. Hwang, T. Hyeon and Y. W. Kim, *Nano Lett.*, 2003, **3**, 1289; (*e*) B. Veisz and Z. Király, *Langmuir*, 2003, **19**, 4817; (*f*) S. U. Son, Y. Jang, K. Y. Yoon, E. Kang and T. Hyeon, *Nano Lett.*, 2004, **4**, 1147.
23. L. A. Gugliotti, D. L. Feldheim and B. E. Eaton, *Science*, 2004, **304**, 850.

24. Y. Xiong, J. M. McLellan, J. Chen, Y. Yin, Z.-Y. Li and Y. Xia, *J. Am. Chem. Soc*., 2005, **127**, 17118.
25. Y. Sun, L. Zhang, H. Zhou, Y. Zhu, E. Sutter, Y. Ji, M. H. Rafailovich and J. C. Sokolov, *Chem. Mater*., 2007, **19**, 2065.
26. H. Kang, Y.-W. Jun, J.-I. Park, K.-B. Lee and J. Cheon, *Chem. Mater*., 2000, **12**, 3530.
27. H.-Y. Lee, S. Ryu, H. Kang, Y.-W. Jun and J. Cheaon, *Chem. Commun*., 2006, 1325.
28. J. Belloni, M. Mostafavi, H. Remita, J. L. Marignier and M. O. Delcourt, *New J. Chem*., 1998, 1239.
29. S. Remita, M. Mostafavi and M. O. Delcourt, *New J. Chem*., 1994, **18**, 581.
30. R. Krishnaswamy, H. Remita, M. Imperor-Clerc, C. Even, P. Davidson and B. Pansu, *ChemPhysChem*, 2006, **7**, 1510.
31. G. Surendran, L. Ramos, B. Pansu, E. Prouzet, P. Beaunier, F. Audonnet and H. Remita, *Chem. Mater*., 2007, **19**, 5045.
32. M. Tréger, C. de Cointet, H. Remita, J. Khatouri, M. Mostafavi, J. Amblard, J. Belloni and R. De Keyser, *J. Phys. Chem. B*, 1998, **102**, 4310.
33. H. Remita, A. Etcheberry and J. Belloni, *J. Phys. Chem. B*, 2003, **107**, 31.
34. H. Remita, I. Lampre, M. Mostafavi, E. Balanzat and S. Bouffard, *Radiat. Phys. Chem*., 2005, **72**, 575.
35. K. Mallik, M. Mandal, N. Pradhan and T. Pal, *Nano Lett*., 2001, **1**, 319.
36. F. Kim, J. H. Song and P. Yang, *J. Am. Chem. Soc*., 2002, **124**, 14316.
37. A. Fukuoka, N. Higashimoto, Y. Sakamoto, S. Inagaki, Y. Fukushima and M. Ichikawa, *Microporous Mesoporous Mater*., 2001, **48**, 171.
38. K. Esumi, A. Suzuki, N. Aihara, K. Usui and K. Torigoe, *Langmuir*, 1998, **14**, 3157.
39. C. Ferradini and J. P. Jay-Gerin, *Radiat. Phys. Chem*., 1996, **48**, 473.
40. J. H. Baxendale and P. J. Wardman, *J. Chem. Soc., Faraday Trans. 1*, 1973, **69**, 584.
41. N. Getoff, A. Ritter, F. Schworer and P. Bayer, *Radiat. Phys. Chem*., 1993, **41**, 797.
42. R. Derai, H. Remita and M. O. Delcourt, *Radiat. Phys. Chem*., 1991, **38**, 483.
43. C. Langhammer, Z. Yuan, I. Zoric and B. Kasemo, *Nano Lett*., 2006, **6**, 833.
44. M. J. Seco, *J. Chem. Educ*., 1989, **66**, 779.
45. N. Tsud, V. Johanek, I. Stara, K. Veltruska and V. Matolin, *Surf. Sci*., 2000, **467**, 169.
46. *Practical Surface Analysis by Auger and X-Ray Photoelectron Spectroscopy*, ed. D Briggs and M. P. Seah, John Wiley & Sons, New York, 1984.
47. J. W. Mullin, *Crystallization*, Butterworth, London, 1961.
48. S. Remita, M. Mostafavi and M. O. Delcourt, *New J. Chem*., 1994, **18**, 581.
49. V. F. Puntes, K. M. Krishnan and A. P. Alivisatos, *Science*, 2001, **291**, 2115.
50. Z. L. Wang, *J. Phys. Chem. B*, 2000, **104**, 1153.




 